

## A HIGH RESOLUTION LUMINOSITY MONITOR FOR SLAC EXPERIMENT E158

G. M. JONES

*Stanford Linear Accelerator Center, 2575 Sand Hill Road, Menlo Park CA 94025*  
*E-mail: markj@slac.stanford.edu*

*(For the E158 Collaboration)*

A calorimetric detector based on ionization has been employed as a low-angle luminosity monitor for the parity violation experiment E158<sup>1</sup> at SLAC. The experiment utilizes a 50 GeV polarized electron beam on a liquid hydrogen target. The detector looks at high energy Mott and Moller scattered electrons, with a per pulse flux of  $4 \times 10^8$  particles. This large signal allows the device to serve the dual role of monitoring target density fluctuations, as well as detecting false asymmetries. In the first physics run of the experiment, the detector has achieved a per-pulse intensity asymmetry resolution of 170 parts per million. The linearity of the device also has been verified to  $\leq 1\%$ .

### 1. E158 Overview

#### 1.1. *Physics Goals*

The electroweak theory has been probed to an astounding level at the  $Z^0$  resonance through the joint contributions of LEP and SLC. The purpose of E158 is to complement these results by measuring the weak mixing angle at a much lower  $Q^2$ . This will allow new insight into the running of  $\sin^2\theta_W$  and form a more complete test of the Standard Model.

Figure 1 is an adaptation of a plot by Czarnecki and Marciano<sup>2</sup> displaying the Standard Model prediction for the running of  $\sin^2\theta_W$ . Here,  $\nu N$  refers to the NuTeV experiment at Fermilab<sup>3</sup>, and APV denotes the result of the atomic parity violation experiment on cesium conducted at the University of Colorado at Boulder<sup>4</sup>. The NuTeV result is actually  $3\sigma$  above the Standard Model. Since the publication of the Boulder experiment, the interpretation of their result has evolved as new theoretical treatments have been applied<sup>5,6,7,8</sup>. In the plot, the APV point is now roughly  $2\sigma$  below the theoretical value<sup>9</sup>.

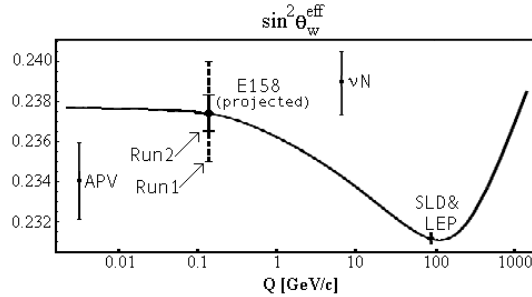


Figure 1. Standard Model running of  $\sin^2\theta_W$

### 1.2. *E158 Layout*

The experiment utilizes a longitudinally polarized electron beam provided by the 50 GeV linac at SLAC on an unpolarized target of liquid hydrogen ( $\text{LH}_2$ ) to measure the parity-violating asymmetry in Moller scattering. Following the target, a dipole chicane and a quadrupole package are used to focus the Moller electron signal onto the main detector. This setup is depicted in Figure 2. From Standard Model calculations<sup>2</sup>, the expected asymmetry for E158 is  $\sim 150$  parts per billion (ppb). Due to the small size of this number, it is extremely important that all sources of false asymmetries be understood and quantified.

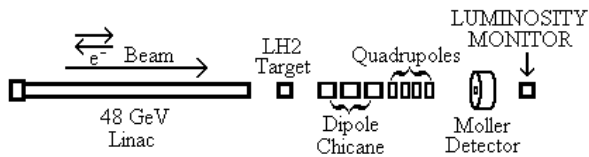


Figure 2.

### 1.3. *Purpose of Luminosity Monitor*

The luminosity monitor (lumi) is located 70 meters downstream of the hydrogen target at an angle of approximately 1 milliradian. From GEANT simulations of a nominal beam rate of  $5 \times 10^{11} e^-$  per pulse, the lumi is expected to see a flux of  $4 \times 10^8 e^-$ . Based purely on counting statistics, this extremely high counting rate sets the scale for the maximum resolution of the detector at the 50 ppm level.

Simulations done at SLAC<sup>10</sup> show that the signal of the lumi is comprised of 70% Mott scattered electrons, with the remaining 30% made up of high

energy Moller electrons. The average energy of these electrons is  $\sim 40$  GeV. In this kinematics region, the theoretical physics asymmetry is only 5 ppb. This is the defining feature of the lumi: it should measure no asymmetry within the proposed statistics of the experiment. This would be a powerful test against the presence of false asymmetries.

## 2. Detector Design

### 2.1. *Concerns and Constraints*

The ultimate design of the lumi was dictated by the strict requirements of E158. The main concern was in keeping the intensity asymmetry resolution at the scale of 100 ppm. For E158, custom 16-bit adcs were constructed on site with noise properties sufficient for the experiment.

Minimizing systematics due to non-linearities was also a concern. Over the full course of the experiment, the charge asymmetry is expected to be at the level of 200 ppb or below. Because of the small size of the Moller asymmetry, it is desirable to keep any individual systematic effect at the 1 ppb level. This translates to a demand on linearity at the 0.5% level.

An interesting requirement on lumi design occurs because of asymmetries found in synchrotron radiation, due to a possible presence of transverse polarization of the electron beam. From simulations, it is known that about 17W of synchrotron radiation hits the lumi, originating mainly from the final dipole magnet of the spectrometer. This is a non-negligible portion of the 150W total signal. Inserting E158 spectrometer parameters into the theoretical formulas<sup>11</sup>, and assuming a transverse beam polarization of 1% nets the conclusion that the contribution to the total detector signal must be less than 1% in order to keep the observed asymmetry on the few ppb level.

The final requirement on the detector design was that it had to be robust against radiation damage. Over the course of the experiment, the detector will get a dose on the order of a gigarad.

### 2.2. *Physical Construction*

The lumi is comprised of 16 individual chambers, arranged into two separate, complementary detectors. These are simply called the "front" and "back" lumi. The front lumi serves as the primary device, while the back lumi is used mainly as a cross-check. Upstream of the front lumi is 7 radiation lengths of aluminum, which performs the dual role of showering the signal and attenuating the synchrotron radiation background. Between the front and back lumi detectors is an additional 4 radiation lengths of aluminum. Figure 3 depicts the full detector layout.

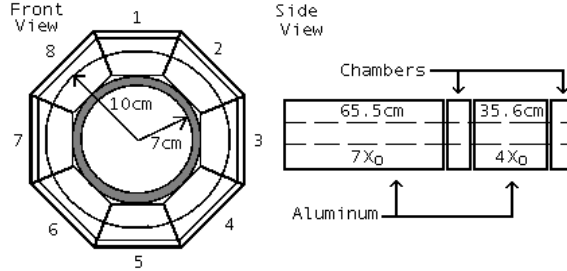


Figure 3.

Inside of each chamber, there are 11 parallel plates, positioned transverse to the beamline. These are alternately kept at 100V and ground, so that when a charged particle traverses the chambers, the electrons it liberates through ionization are collected. A signal is actually read out from each plate in the device, since they are all capacitively coupled. By reading in the signals differentially, noise pickup from the cables is reduced.

The separation between the plates is approximately one millimeter. This small distance was chosen to ameliorate possible non-linearities induced by unwanted recombination of liberated electrons and ions in transit to the plates. The buffer gas was chosen to be nitrogen, since it provided adequate signal sizes and did not require the special attention required by a flammable gas.

Simulations in EGS show that the front degrader produces a  $\times 40$  amplification of the incident signal. The 1cm of nitrogen gas in each chamber also produces a similar amplification factor. The signal sizes seen from a single front chamber for typical running conditions are between 4 to 8 volts. This allows the detector to be run entirely without amplifiers.

The ratio of the observed signals in the front to the back lumi is about 3:1, which agrees with the simulations. Since the back chamber has a much reduced signal, it can serve as a linearity check on the front ring of chambers. The fact that the front and back rings of the detector measure the same signal flux allows the back chambers to be a crosscheck for the front chambers for the measured asymmetries as well.

### 3. Detector Performance

#### 3.1. Resolution

The ultimate per-pulse intensity asymmetry resolution achieved during the first run of E158 was at the level of 170 ppm for the front ring of the detector, and 250 ppm for the back ring.

To achieve this level of resolution, it was necessary to remove beam related

effects from the detector signal. This is accomplished by finding the slope of the correlation between asymmetries in the detector and a beam position monitor (bpm) and then subtracting out this relation. After implementing these corrections, the detector becomes less sensitive to beam parameters and approaches its maximum possible resolution. For E158, seven individual bpms are used to remove the dependence on x and y position and angle on target, as well as energy related effects.

Before this regression procedure is done, it is common for the raw resolution of the front detector to be at the 250 ppm level, while the back was often near 425 ppm.

By noting the sensitivity of the detector to fluctuations in these beam parameters, and the corresponding resolution on that parameter provided by the bpms, the predicted final regressed resolution of the detector can be calculated. In this way, all sources of noise for the detector can be itemized. It should be noted that the bpms for E158 attained an excellent position resolution, at the level of 2 microns.

Taking into account the noise contributions from bpm and toroid resolution, as well as including counting statistics and pedestal fluctuations, it is found that the resolution of the detector should be 110 ppm. This is significantly below the observed 170 ppm, pointing to an unknown noise source around the level of 100 ppm.

The source of this extra noise contribution is still unidentified, though a likely candidate is electronics crosstalk. It has been observed that the resolution of the detector is greatly affected by adjusting timing parameters on the adcs. The 170 ppm resolution is only achieved for a very specific timing setting. For most other settings, the resolution worsens to 280 ppm. Research into the implications of this is still ongoing.

### **3.2. Linearity**

Conceptually, the linearity of a detector is a simple parameter. In practice, however, determining the linearity of the luminosity monitor to the level of 0.5% has proven to be quite a challenge. Though several methods have been employed, the most promising technique involves making cuts on beam parameters below bpm resolution and then plotting lumi asymmetry (not normalized by toroid) vs. toroid asymmetry. By making tight cuts, and working with asymmetries, the large effects coming from beam motion are mitigated. About 0.1% of the data survives this cut. The deviation of the observed slope from unity is then a direct measure of the linearity of the lumi-toroid system. Figure 4a shows the slopes obtained from this method for each chamber in the front ring of the lumi. Clearly, there is still a systematic effect related

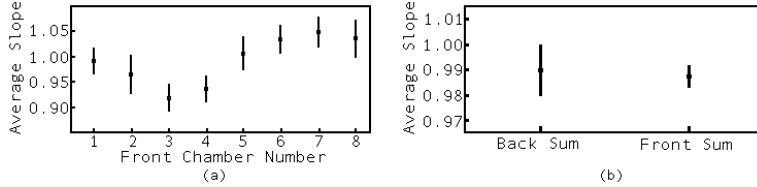


Figure 4. A slope of 1 indicates 100% linearity. Notice the azimuthal dependence to the observed slopes in 4a.

to position, since the azimuthal dependence is quite pronounced. One way to decrease this effect is to sum up an entire ring of the detector, and perform the same analysis. Since the gain of each chamber is essentially identical, by summing the full azimuth of a ring, position effects are greatly reduced. The suppression in sensitivity is seen to be at least factor of 10. This is quantified by comparing the response of a single chamber to that of an entire ring for a given deviation in a beam parameter. Figure 4b shows the results obtained by employing the same method as before on an entire ring of chambers.

The error bar in the plot comes purely from the fit of the slope between lumi asymmetry and toroid asymmetry. As an estimate of the remaining systematic effect due to beam position fluctuations, we note that the amplitude of the azimuthal oscillation in the Figure 4a was about 8%. With the order of magnitude in beam sensitivity suppression afforded by the sum, this brings the systematic error down to about 1%. The front and back rings are both consistent with being linear, then, with the slope of the front ring found to be  $0.987 \pm 0.004(\text{stat}) \pm 0.010(\text{syst})$ .

### 3.3. Synchrotron Radiation

To set an upper limit on the fraction of the detector signal coming from synchrotron radiation, the average signal size is compared with the target in and out of the beam. Figure 5 shows the ratio of these two configurations, on a per chamber basis. All chambers show that the maximum background is below the 1% level required by the experiment. Moreover, since chambers 3 and 7 are in the horizontal plane (the bend plane of the last spectrometer dipole magnet), the amount of synchrotron radiation they receive is orders of magnitude above the other chambers. It is precisely these chambers that show a pronounced spike in the above plot. Therefore the actual synchrotron background is more appropriately quantified as the height of these spikes above the level of the other chambers. The synchrotron background is then demonstrated to be well below the 1% requirement.

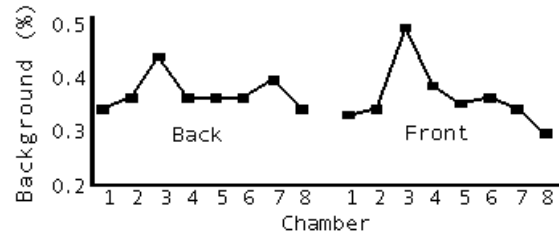


Figure 5. The ratio of average signal with target out to target in, versus channel number

### 3.4. Target Density Fluctuations

Pulse-to-pulse target density fluctuations would present themselves as a correlation between the Moller and Lumi detectors. This is due to the fact that each detector has a sufficiently unique signal flux that the only real connection between them is the target itself. Figure 6 displays the Moller detector asymmetry vs. the lumi asymmetry. No significant amount of target density

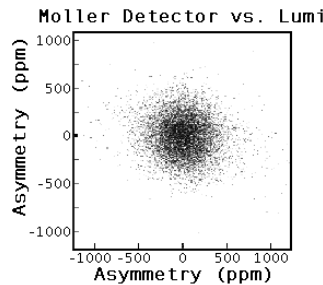


Figure 6. There is no correlation between the two detectors.

fluctuations are observed.

### 3.5. Lumi as a BPM

Because the individual chambers of the lumi are exceptionally well gain matched, the detector was able to be used like a bpm for alignment purposes. The beam position is figured from a "center of mass" type calculation, using the signal size in each chamber as the mass, and the chamber position in space as the weighting factor. For deviations of less than a few centimeters from the center of the detector, this was found to be accurate to better than 1mm. Figure 7 shows the calculated beam position in the front lumi ring, vs. different angle setpoints of the beam on target. They indicate that the beam would be centered in the front ring of the detector for the X-angle set to  $6\mu\text{R}$  and the

Y-Angle set to  $0\mu\text{R}$ . This extra feature of lumi, derived from the simple nature

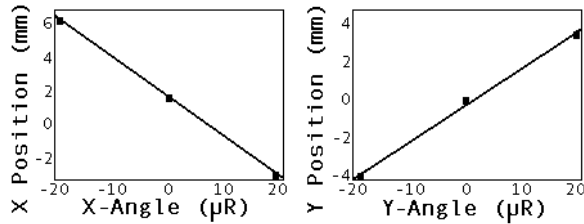


Figure 7.

of the detector, assisted in the initial positioning of the E158 beam.

#### 4. Conclusion

The luminosity monitor for E158 has proven to be a powerful, yet simple detector. The device has shown an exceptional per-pulse intensity asymmetry resolution of 170 ppm. The linearity of the device had been demonstrated at the 1% level for the first run of the experiment. The background contamination of synchrotron radiation has been shown to be at an acceptable level. The detector has been critical in looking for target density fluctuations. As more data from the first run of E158 is processed, the lumi will become an important monitor for false asymmetries.

For the final run of E158, the goals will be to better understand the relation of the adc electronics to resolution and to demonstrate linearity to 0.5%.

#### References

1. K. S. Kumar et al., [Online] Available: <http://www.slac.stanford.edu/exp/e158/documents/proposal.ps.gz>, (1997).
2. A. Czarnecki and W. Marciano, *Int. J. Mod. Phys.* **A15**, 2365 (2000).
3. G. P. Zeller et al., *Phys. Rev. Lett.* **88**, 091802 (2002).
4. C. S. Wood et al., *Science* **275**, 1759 (1997).
5. C. S. Wood et al., *Can. J. Phys.* **77**, 7 (1999).
6. S. C. Bennett and C. E. Wieman, *Phys. Rev. Lett.* **82**, 2484 (1999).
7. A. Derevianko, *Phys. Rev. Lett.* **85**, 1618 (2000).
8. V. A. Dzuba et al., [Online] Available: <http://xxx.lanl.gov/abs/hep-ph/0111019>, (2001).
9. V. A. Dzuba et al., [Online] Available: <http://xxx.lanl.gov/abs/hep-ph/0204134>, (2002).
10. L. Keller, [Online] Available: <http://www.slac.stanford.edu/exp/e158/documents/technotes/LUMIAcceptance.ps.gz>, (2001).
11. A. Bondar and E. Saldin, *Nucl. Instr. Meth.* **195**, 577 (1982).